Infrared Spectrograph
Technical Report Series

IRS-TR 11001: Temporal Responsivity Variations on the Red Peak-Up Sub-Array

G.C. Sloan (1) & D.A. Ludovici (2) *

3 August, 2011

Abstract

Over the course of the cryogenic mission of the *Spitzer Space Telescope*, the responsivity of the Red Peak-Up sub-array on the Infrared Spectograph (IRS) varied by $\sim$2%, based on an analysis of five standard stars. The sensitivity dropped 1.7% after the first 14 IRS campaigns, then climbed back up 1.0% later in the mission. The uncertainty in these measurements is better than $\sim$0.3%. The random variations in the Peak-Up photometry of the standard stars has a gaussian distribution of width $\sim$2%, similar to the magnitude of the systematic temporal variations.

1 Introduction

The cryogenic mission of the *Spitzer Space Telescope* (Werner et al. 2004) lasted from August 2003 to May 2009. In that time, the Infrared Spectrograph (IRS; Houck et al. 2004) made repeated observations of several standard stars. Those fainter than $\sim$ 1 Jy at 12 μm could be observed both spectroscopically and on the Peak-Up (PU) subarrays on the Short-Low (SL) module. It was highly desirable

*(1) Infrared Spectrograph Science Center, Cornell University, (2) Department of Physics, West Virginia University; NSF REU Research Assistant, Astronomy Department, Cornell University

to do so for two reasons. First, using the target for self peak-up reduced the likelihood of possible pointing errors, because as long as the coordinates were good to within several arcseconds, the on-board PU algorithm would find the source and shift it with its full precision to the center of the spectrographic slits. With an offset star, any errors with the coordinates of *either* star translated into a pointing error. Second, the PU observations gave us an independent photometric measurement of the target, allowing us to monitor the stability of both the standard stars and the instrument. If a standard varied in isolation compared to the others, then it probably is a variable star. If all of the standards varied in concert, variation in system response is the likely culprit.

2 Observations

Table 1 lists the five stars observed most frequently with the Red Peak-Up subarray during the cryogenic *Spitzer* mission. These stars were faint enough to not saturate the Red PU array, which would have resulted in poorer pointings for spectroscopy, and they were brighter than $\sim$ 150 mJy at 16 μm. For stars below this limit, we used the Blue PU sub-array, which gave slightly more accurate pointings due to the smaller point-spread function (PSF). Figure 1 illustrates the responsivity of the two PU sub-arrays, which peak at approximately 16 μm (Blue) and 22 μm (Red), along with the actual spectra of the standards considered here.

Table 1—Peak-Up Acquisition Observations

Standard star	**Spec. class**	**Observed in campaigns**	**Self-PU AORs**	**Red PU images rejected**	**used**
HR 6348	K1 III	P–61 (intermittently)	84	5	163
HD 166780	K4 III	P–61 (intermittently)	41	3	79
HD 173511	K5 III	5–61	132	9	217
α Lac	A1 V	1–58 (intermittently)	28	2	54
δ UMi	A1 V	P–19 (intermittently)	43	3	83

The PU data were obtained in two sets of three consecutive images, which were read using double-correlated sampling and then combined and analyzed on the spacecraft. After the first set, or "acquisition" set, the centroid was determined and the telescope moved to shift the target to a well-calibrated portion of the PU array known as the "sweet-spot". The three "sweet-spot" images were then combined and analyzed as before. The second centroid was then used to shift the

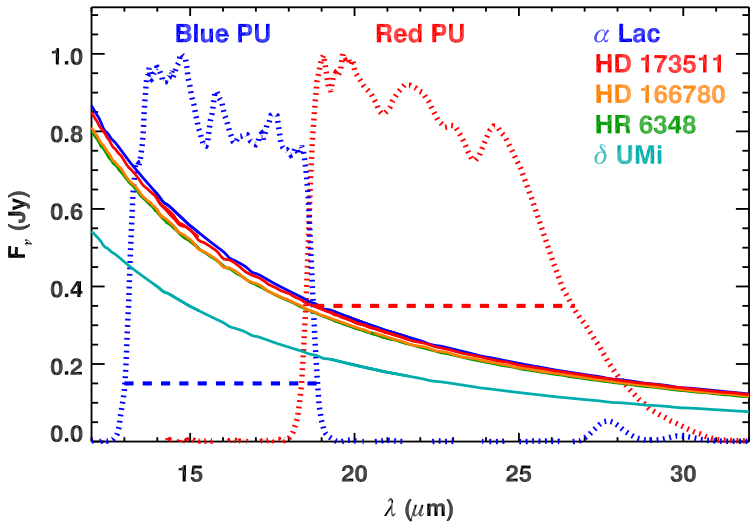

Figure 1 —The normalized responsivities of the Blue and Red PU sub-arrays, for a bias voltage of 2.0 volts, as operated during the *Spitzer* mission (dashed curves). The horizontal dashed lines show the photometric levels at which the PU sub-arrays begin to saturate. Spectra of the five standards considered here are also plotted.

target to the first requested spectroscopic slit. Thus, each PU observation results in two combined images and two independent photometric measurements.

Early in the mission, we were very conservative about saturating any pixels in the PU sub-arrays, which would reduce the accuracy the centroiding algorithm and introduce possible pointing errors. Consequently, the observations of HD 173511 used offset PUs through IRS Campaign 4, and the corresponding astronomical observing requests (AORs, 20 in all) have no PU photometry for this source.

3 Analysis

The analysis begins with S18.18 pipeline output from the *Spitzer* Science Center (SSC). We use the "acqr.fits" files, which are more processed than the raw "bcd.fits" files available in previous pipeline versions. The "bcd" images can suffer from what is known as "jailbarring". The images are read one row of 128 pixels at a time, with 32 reads of four-pixel groups by four parallel analog-to-digital converters (ADCs). Sometimes the dark current from the four ADCs drifts, resulting in vertical stripes in the images. The "acqr" images delivered by the SSC correct this artifact.

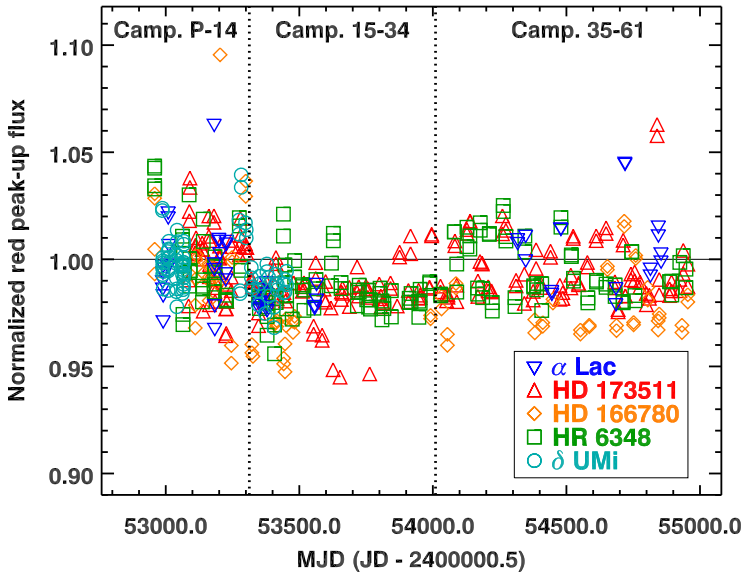

Figure 2 —The photometry of the five standards most frequently observed in the Red PU subarray, normalized to their mean response in the period from Campaigns P through 14. The responsivity drops ∼2% during the middle portion of the cryogenic mission and then climbs ∼1% climb in later campaigns. The vertical dashed lines separate the individual campaigns into the three sets we use to correct the photometry for these systemic shifts. (MJD = modified Julian date = JD − 2400000.5.)

Table 2—Normalized Mean Photometry

Target	Campaigns	N	mean	σ	u
HR 6348	P–14	37	1.0	0.0187	0.0031
	15–34	64	0.9840	0.0106	0.0013
	35–61	62	0.9849	0.0134	0.0017
HD 166780	P–14	24	1.0	0.0291	0.0059
	15–34	19	0.9649	0.0085	0.0019
	35–61	36	0.9784	0.0142	0.0024
HD 173511	P–14	52	1.0	0.0158	0.0022
	15–34	78	0.9845	0.0119	0.0013
	35–61	87	0.9784	0.0153	0.0016
α Lac	P–14	24	1.0	0.0190	0.0039
	15–34	12	0.9820	0.0046	0.0013
	35–61	18	1.0060	0.0183	0.0043
δ UMi	P–14	56	1.0	0.0124	0.0017
	15–34	25	0.9872	0.0069	0.0014
	35–61	0	.....	.....	.....
Combined mean	P–14	193	1.0	0.0181	0.0013
	15–34	198	0.9826	0.0103	0.0007
	35–61	203	0.9929	0.0149	0.0010

We combined the three images from one position using median filtering, and then measured the signal from the target using simple aperture photometry in two ways. We use a narrow aperture of radius four pixels and a corresponding sky radius of eight pixels, and a broad aperture of radius seven pixels with a sky radius of 14 pixels. In both cases, the sky is measured in the outer annulus and removed from the photometry inside the inner circle. The two apertures produce similar results, but because the photometry in the narrow apertures shows less noise, we concentrate on those results here.

In rare cases, the photometry from the "acquisition" and "sweet spot" images disagree with each other, most likely because of latent images in the SL detector from previous observations. In those cases, the acqusition image is far more likely

to produce spurious results. We have filtered the data by using only the second (sweet-spot) image when the difference between the two images is greater than 1.5% of their mean. As a result, only a handful of data remain outside an envelope of $\sim \pm 5\%$.

Figure 2 illustrates the resulting photometry, normalized for each source to its mean over the period from Campaign P in the Science Verification (SV) phase to Campaign 14 during normal operations. All five stars follow the same trend of a decline in signal of $\sim$2% from early in the mission to about half-way through, followed by a slight $\sim$1% increase in signal from then to the end of the cryogenic mission. Because all five stars vary in unison, we conclude that we are dealing with variation in the system. We will assume that the issue is a subtle change in responsivity. Any additive offset would have been removed by the sky subtraction.

The spread in the data at any given time is on the order of a few percent, about as large as the apparent trends. Consequently, we do not attempt any kind of polynomial fit to the responsivity as a function of time. Instead, we have separated the cryogenic mission into three phases, each containing approximately equal numbers of photometric measurements and corresponding roughly to the overall breaks in the apparent trends.

Table 2 presents the means for each standard for the three phases of the mission, the standard deviation (σ) and the uncertainty in the mean ($u = \sigma/\sqrt{N}$). The last set of data in the table gives the combined means of all five standards during the mission, weighted to account for the number of observations. Our overall photometric uncertainty is $\sim$0.1%, compared to shifts in system responsivity of 1.7% down in the middle campaigns and 1.0% back up for later campaigns.

4 Discussion

Based on this analysis, we recommend divisive corrections to Red PU photometry of 0.9826 ($\pm$0.0007) for IRS Campaigns 15–34 and 0.9929 ($\pm$0.0010) for IRS Campaigns 35–61. These corrections bring all data into line with the early IRS campaigns. For most users of the IRS, this level of precision for red PU photometry is probably unnecessary, but we will apply these corrections in future technical reports and papers describing the spectrophotometric calibration of the IRS and its application to the sample of spectroscopic standards observed during the cryogenic mission.

Ludovici et al. (2011) presented an earlier analysis using S18.7 data at the AAS meeting in Seattle. They found corrections within $\sim$0.5% of the values

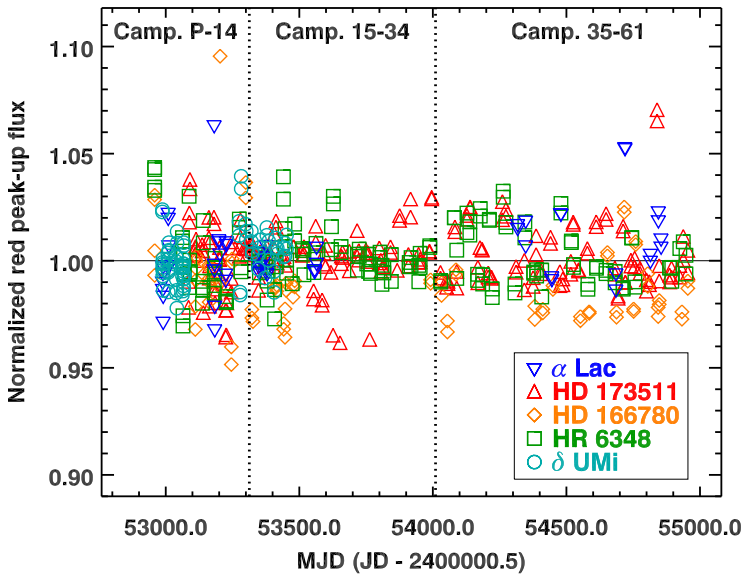

Figure 3 —The Red PU photometry of the five standards from Fig. 2, after applying the recommended corrections upward of 1.70% for Camp. 15–34 and 0.70% for Camp. 35–61.

presented here with different filtering for outliers and slightly different breaks between campaigns (the middle group was Camp. 16–34). Analysis of the S18.7 data more consistent with the steps described in Section 3 produce results within ∼0.15–0.3% of our recommended corrections above, depending on the detailed assumptions. These differences give a reasonable estimate in our uncertainty.

Table 3—Detrended means

Target	Detrended mean
HR 6348	1.0013 ± 0.0011
HD 166780	0.9890 ± 0.0023
HD 173511	1.0015 ± 0.0010
α Lac	1.0043 ± 0.0024
δ UMi	1.0014 ± 0.0012

Figure 3 illustrates the impact of the recommended corrections on the data. The overall trends apparent in Figure 2 have largely been removed. Table 3 presents the detrended means for the five standards. The means were determined after the data were first normalized to the signal for each star in Campaigns P–14, then detrended with the recommended divisive corrections given above (0.9826

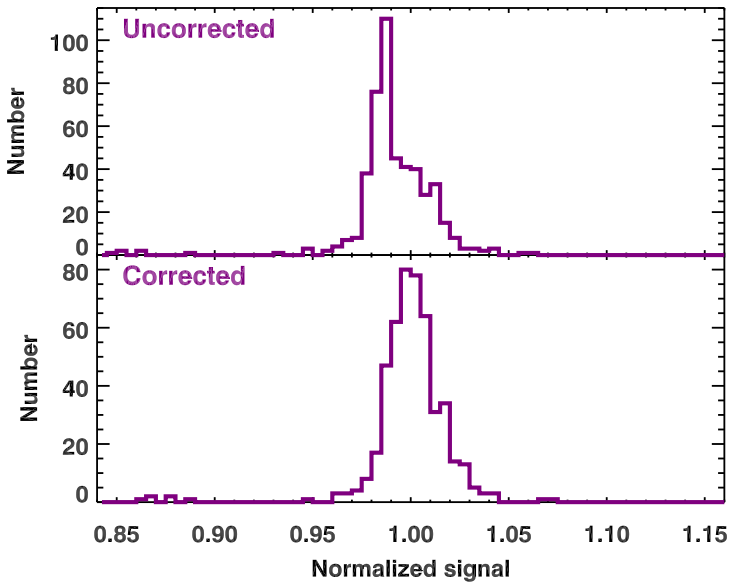

Figure 4 —The combined Red PU photometry for HR 6348, HD 173511, and δ UMi after normalizing the data for each source to the mean of Campaigns P–14. The top panel shows the PU signals before we have corrected the data from later campaigns for the temporal responsivity variations. The bottom panel shows the effect of the correction. The data plotted in this figure include outliers filtered from previous analysis.

and 0.9929). For three standards (HR 6348, HD 173511, and δ UMi), the difference between the corrected means and unity are close to the uncertainty in the mean.

For HD 166780, however, the mean is 0.989, which is a more significant difference. Comparing the data up to and after Campaign 14, we have 1.0 ± 0.0059 vs. 0.9843 ± 0.0017, which is a difference of 0.0157 ± 0.0061, indicating a 1.6% drop in emission over the *Spitzer* mission with a 2.6-σ level of confidence. We cannot claim conclusively that HD 166780 is a variable star, but this change in flux does raise some concerns.

The photometric behavior of α Lac is also troublesome, but while a similar analysis suggests a 0.7% increase in brightness, the confidence level is only 1.3 σ, making it impossible to draw any conclusions.

Figure 4 illustrates how the corrections improve the distribution of the Red PU photometry from the three most stable sources: HR 6348, HD 173511, and δ UMi. The histograms include *all* of the data from these three sources, including the images filtered in the analysis above (by rejecting the acquisition image when

it disagrees with the sweet-spot image by more than 1.5%). The lower distribution is clearly more gaussian in behavior, even if the standard deviation has improved only slightly, from 2.2% to 2.0%. This random distribution is similar in spread as the more systematic temporal variations measured above.

References

Houck, J.R., et al. 2004, *ApJS*, **154**, 18.

Ludovici, D., Sloan, G.C., Barry, D.J., Lebouteiller, V., Bernard-Salas, J., & Spoon, H.W.W. 2011, "Characterization and Calibration of the Infrared Spectrograph on the *Spitzer Space Telescope*," *BAAS*, Abstract 254.22.

Werner, M.W., et al. 2004, *ApJS*, **154**, 1.